RSC Advances

PAPER

View Article Online
View Journal | View Issue



Cite this: *RSC Adv.*, 2018, **8**, 36910

# Room temperature two-photon-pumped random lasers in $FAPbBr_3$/polyethylene oxide (PEO) composite perovskite thin film†

Long Xu, ‡[a] Yan Meng,‡[a] Caixia Xu*[b] and Ping Chen*[a]

Solution-processed organic–inorganic halide lead perovskites have attracted increasing attention due to their great potential in low-cost, effective, and versatile light emission applications and large-scale portable optoelectronic devices. In this paper, formamidinium lead tribromide perovskite thin films composited with polyethylene oxide (PEO) were fabricated by a solution processing method. Great enhancement of photoluminescence was observed and more attractively, two-photon-pumped random lasing action could be achieved at room temperature when pumped by a nanosecond pulse laser with excitation wavelength centered at 1064 nm. Evident transition from spontaneous upconversion emission to random lasing action was investigated by monitoring the log–log light emission slope and peak width at half height. The lasing threshold is at around 1.1 mJ $cm^{-2}$, which is comparable to that of other two-photon upconversion random lasers. The efficient random lasing emission originates from the multiple random scattering provided by the micrometer-scale rugged morphology and polycrystalline grain boundaries. Compared with conventional lasers that normally serve as a coherent light source, the perovskite random lasers show promise in fabricating low-cost thin-film lasing devices for flexible and speckle-free imaging applications.

Received 6th September 2018
Accepted 22nd October 2018

DOI: 10.1039/c8ra07452f

rsc.li/rsc-advances



## Introduction

Recent years have witnessed the great development of low-cost and effective organic light emitting diodes,[1] solar cells,[2] field-effect transistors[3–6] and other optoelectronic devices,[7] which benefit from the high-performance of hybrid organic–inorganic halide lead perovskites.[8–13] In general, these types of materials exhibit outstanding optical and electrical properties, such as high carrier mobility,[14] spectrally tunable optoelectronic property[15] and high fluorescence yield,[16] which are desirable for designing low-threshold lasers[17] and photodetectors.[18] From the perovskite microlaser aspect, solution-processed methylammonium lead halide perovskite ($MAPbX_3$, X = Cl, Br, I) and cesium lead halide perovskite ($CsPbX_3$) quantum dots, particularly in single crystal forms, possess large absorption coefficients, long carrier lifetimes and low trap densities, giving rise to low-threshold and tunable optically-pumped lasing and photoluminescence with high quantum efficiency.[19–21] Compared with classic inorganic semiconductors and colloidal quantum dots, one fatal flaw of $MAPbX_3$ and $CsPbX_3$ perovskites is that they are too fragile to exhibit stable performance because of their poor thermal and high humidity sensitivity, which hinder their potential in the realization of sustained inversion and continuous wave pumped lasers. Recently, formamidinium lead halide perovskites ($FAPbX_3$) showed better temperature and moisture stability by converting from methylammonium to formamidinium ($(CH(NH_2)_2^+)$).[22,23] Recently, nanowire lasers of $FAPbX_3$ perovskite with improved stability have been achieved, which stemmed from their unexpected long carrier dynamics and diffusion length.[24,25] Moreover, organic cations and additives also optimized the morphology and photoluminescence of $FAPbX_3$ films.[26] Until now, amplified spontaneous emission, lasers, random lasers, and photoluminescence have been widely studied in $MAPbX_3$, $FAPbX_3$, and $CsPbX_3$ perovskite thin films and bulk.[27–34] Although many practical light sources made by halide lead perovskite crystals have already been reported, two-photon excitation-pumped lasers possess advantages that cannot be replaced by the former. For example, in the application of the non-destructive detection and imaging of biological tissues, two-photon pumping technology can avoid damage to organisms by irradiating near-infrared light sources with minor absorption on the surface of the biological tissue. By increasing the pumping intensity, two-photon- or three-photon-pumped photoluminescence and lasing action in these materials have also been observed. However, only a few of them could be

[a]School of Physical Science and Technology, Southwest University, Chongqing, 400715, China. E-mail: chenping206@126.com

[b]School of Primary Education, Chongqing Normal University, Chongqing, 400700, China. E-mail: noendness@126.com

† Electronic supplementary information (ESI) available. See DOI: 10.1039/c8ra07452f

‡ These authors contribute equally to this work.

accomplished at room temperature because of their thermal stabilities.[35,36] Considering perovskite thin films in solution, it is also very essential and highly desirable to develop a stable two-photon-pumped hybrid lead halide perovskite laser at room temperature. In this study, two-photon-pumped photoluminescence and random lasing action were achieved in formamidinium lead tribromide perovskite ($FAPbBr_3$) thin films when composited with a polyethylene oxide (PEO: H–[–O–$CH_2$–$CH_2$–]$_n$–OH) additive under the pumping of a nanosecond pulse laser with excitation wavelength centered at 1064 nm. Evident transition from spontaneous upconversion emission to random lasing action was investigated by monitoring the log–log light emission slope and narrowed peak width at half height. Compared with conventional lasers that normally serve as a coherent light source, the perovskite random lasers are promising in fabricating low-cost thin-film lasing devices for flexible and speckle-free imaging and projection applications.

## Materials preparation

The precursor solution of $FAPbBr_3$ was prepared in a glove box (water and oxygen content <0.1 ppm). $CH(NH_2)_2Br$ and $PbBr_2$, bought from Xi'an Baolite Optoelectronic Technology Co. LTD, were dissolved in *N*,*N*-dimethylformamide (DMF, Shanghai Aladdin Biochemical Technology Co. LTD., purity > 99.8%) at a concentration ratio of 1.5 : 1. After stirring the solution for more than 12 hours at room temperature, 40 wt% $FAPbBr_3$ solution was obtained. Polyethylene oxide (PEO, Aldrich, average $M_v$ – 1 000 000) was also independently dissolved in DMF solution with a concentration of 20 mg $mL^{-1}$. Finally, PEO solution was mixed with $FAPbBr_3$ precursor solution with a volume ratio of PEO : $FAPbBr_3$ = 10 : 1. For comparison, the same $FAPbBr_3$ precursor solution without PEO solution was also prepared.

Before preparation of the thin films, the quartz substrates were cleaned using an ultrasonic cleaner, and the cleaned quartz substrate was then treated with ultraviolet ozone for 15 min (SunMonde $UVO_3$ Cleaner, 120 W). The PEDOT:PSS film was first coated to the quartz substrate *via* a spin-coating method (4500 rpm, 40 s) to improve the thin film quality. Then, the quartz substrates with the PEDOT:PSS films were transferred to the heating stage in the atmospheric environment to conduct thermal annealing treatment at 120 °C for 20 minutes. After the quartz substrates were cooled, $FAPbBr_3$ and $FAPbBr_3$/PEO composite perovskite nanocrystal films were synthesized by the solution-processed one-step precipitation method (3000 rpm, 60 s) in the glove box. After annealing treatment at 80 °C for 20 minutes, we finally obtained the $FAPbBr_3$ and $FAPbBr_3$/PEO composite perovskite thin films, as seen in Fig. 1(c).

The surface appearance of the as-prepared $FAPbBr_3$ and $FAPbBr_3$/PEO composite perovskite nanocrystal films were characterized by scanning electron microscopy (SEM, JEOL JSM-7100F). The SEM accelerating voltage used in this study was 10 kV and the emission current was 105 μA. As seen in Fig. 1(d), $FAPbBr_3$ perovskite nanocrystals were synthesized; the nanocrystals were spaced closely with a grain size of about 200 nm.

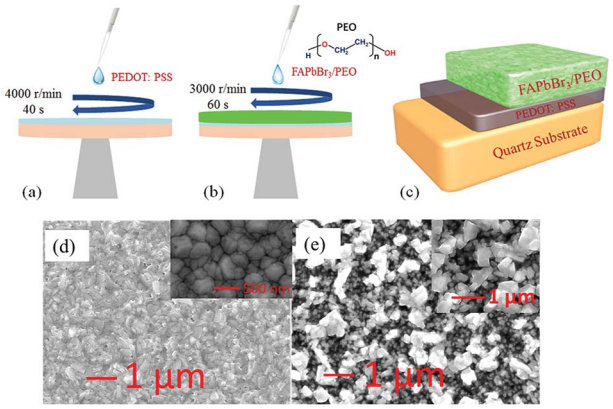


Fig. 1 (a) The preparation of PEDOT:PSS layer by a solution-processed one-step precipitation method; (b) the preparation of $FAPbBr_3$ or the $FAPbBr_3$/PEO layer by a solution-processed one-step precipitation method; (c) schematic of the structure of the prepared specimens; (d) surface appearance image of $FAPbBr_3$ perovskite thin film taken by scanning electron microscope (the inset is also the surface appearance shown at a higher magnification); (e) surface appearance image of $FAPbBr_3$/PEO composite perovskite thin film taken by scanning electron microscope (the inset is also the surface appearance shown at a higher magnification).

The perovskite nanoparticles in the film were tightly arranged before mixing with the PEO molecules. However, on mixing with the PEO molecules, the perovskite nanoparticles in the film are aggregated onto a series of independent islands and are covered by PEO molecules, as seen in Fig. 1(e). These islands formed a covering layer to gather part of the $FAPbBr_3$ perovskite nanocrystals together to form larger units, which effectively protected the $FAPbBr_3$ perovskite nanocrystals from moisture damage and improved the stability of the perovskite thin films.

## Experimental results and discussion

To study the optical properties of the $FAPbBr_3$ and $FAPbBr_3$/PEO composite perovskite thin films, their room-temperature ground-state absorption spectra were measured using a UV-Vis spectrometer (Shimadzu, UV-2600), as seen in Fig. 2(a). The absorption intensity of the $FAPbBr_3$/PEO composite thin films enhanced slightly in the visible region, but increased in the range from 20% to 100% in the UV region. Two main factors contributed to the enhancement of the absorbance of the composite film in the UV region. One factor is that the PEO polymer additive itself very strongly absorbs ultraviolet light, and it increased the absorption of ultraviolet light of the material when it was added to the perovskite thin films. The other factor is that the PEO polymer increased the scattering intensity of the material surface, which in turn increased the resident length of the UV light in the material, which was similar to the increase in the effective distance that photons propagated through the material. When the thin films were pumped with radiation by a violet-blue diode laser at 405 nm with a pumping power of 100 mW (FC-D-405, Changchun New Industries Optoelectronics Technology Co., Ltd), the thin film composited with PEO showed a 10-fold enhancement in the photoluminescence intensity (see the black and red dash lines

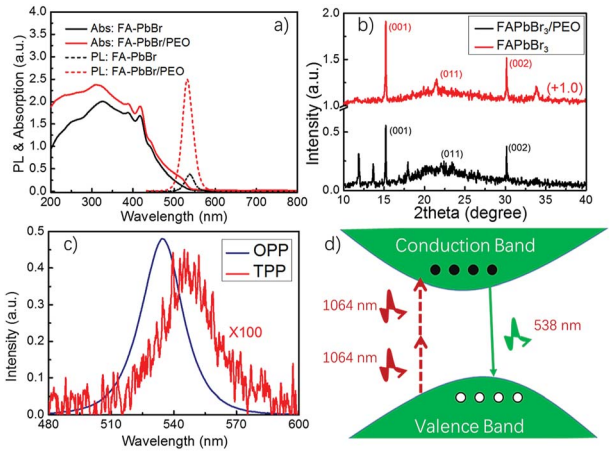


Fig. 2 (a) The room-temperature ground-state absorption and photoluminescence spectra of $FAPbBr_3$ and $FAPbBr_3$/PEO composite perovskite thin films; (b) the X-ray diffraction spectra of $FAPbBr_3$ and $FAPbBr_3$/PEO composite perovskite thin films; (c) one-photon-pumped (OPP) and two-photon-pumped (TPP) photoluminescence of light in $FAPbBr_3$/PEO composite thin films; (d) schematic of the energy transition of the two-photon-pumped photoluminescence process.

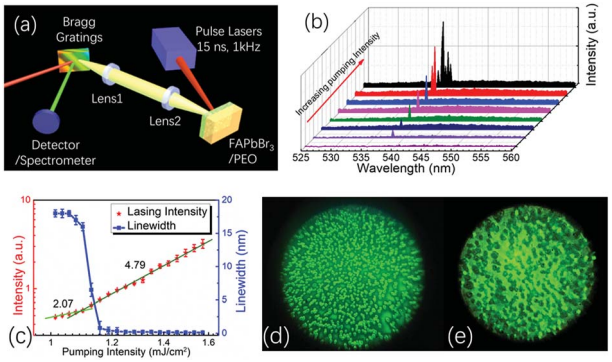


Fig. 3 (a) Illustration of the experimental setup; (b) two-photon-pumped random lasing spectra *versus* pumping intensity; (c) two-photon-pumped random lasing intensity and full width at half maximum intensity *versus* pumping intensity; (d) the TPP photoluminescence and (e) random laser intensity distributions recorded by a home-built fluorescence microscope.

in Fig. 2(a)). The XRD data of these thin films were detected by an X-ray diffractometer (D/MAX-rB, Rigaku, Japan), as shown in Fig. 2(b). The strong (001) and (002) diffraction peaks implied that the composite of $FAPbBr_3$ nanocrystals wrapped in PEO preserved good perovskite structure, albeit it showed some other diffraction peaks. In addition, the one-photon-pumped (OPP) and two-photon-pumped (TPP) photoluminescence in the $FAPbBr_3$/PEO composite thin films were investigated, as seen in Fig. 2(c). Compared with the OPP light emission intensity, the TPP light emission intensity was much weaker because this emission process needs to absorb two photons at 1064 nm continuously to excite the electrons to the conduction band from the valence band (refer to Fig. 2(d)). Hence, TPP photoluminescence would be more ineffective than OPP photoluminescence. While considering the perovskite thin films in solution, it is still very essential and highly desirable to develop a stable and effective two-photon-pumped hybrid lead halide perovskite laser at room temperature.

$FAPbX_3$ perovskite nanowires have exhibited high-performance lasing action by the one-photon-pumped method, which possessed a stable lasing emission for more than $10^8$ laser shots at room temperature.[24] To further study the lasing performance in $FAPbX_3$ perovskite nanocrystals, in this paper, we studied the two-photon-pumped random lasing action in the $FAPbBr_3$/PEO composite thin films. A nanosecond pulse laser with excitation wavelength at 1064 nm (15 ns, 1 kHz) was used as the pumping source, as seen in Fig. 3(a), and the lasing emission was collected by a lens system and separated from the pumping light by using Bragg gratings. In addition, the lasing spectra were measured and recorded by using the spectrometer and its software (Ocean Optics, QE65Pro). All these experiments were conducted at room temperature (20 °C).

Below the threshold, the light emission showed a broad spectrum with the full width at half maximum intensity (FWHM) at around 17 nm, as shown in Fig. 2(b), and the emission peak showed a 13 nm red-shift compared with that in the OPP photoluminescence spectrum. In this region, the emission peak intensity increased along with the pumping energy with a log–log slope of 2.07 (refer to Fig. 3(c)). At this time, the light intensity distribution is homogeneous, as seen in the photograph taken by a home-built fluorescence microscope (Fig. 3(d)). Above the threshold, a sharp peak located at 538.2 nm appeared at the left side of the light emission spectrum (refer to Fig. 3(b)), and the FWHM dropped to 0.4 nm rapidly, which is a remarkable feature of the formation of random lasing action in the specimen.[37] At this time, the log–log slope of laser emission intensity *versus* the pumping intensity increased to 4.79, as seen in Fig. 3(c). Moreover, the light intensity distribution of the random laser was inhomogeneous and concentrated in some localized region, as recorded in Fig. 3(e). Upon further increasing the pumping energy, more lasing modes appeared near the first lasing mode due to the formation of the weak localization of light in a different scattering region. The $Q$ factor of this lasing emission mode could reach up to 1280, which is comparable to the lasing emission from the whispery gallery mode and from nanowires of perovskite materials.[38,39]

To further study the TPP random lasing performance in $FAPbBr_3$/PEO composite perovskite thin films, the polarization property of the lasing emission at 538.2 nm was measured, as shown by the black dots in Fig. 4(a). The largest light emission intensity was observed when the analyser angles were 0° and 180°, while the minimum light emission intensity was observed at the angles of 90° and 270°, which effectively fitted the linear polarization intensity angular distribution, as seen by the red dots in Fig. 4(a). However, the polarization performance of the light emission was still not good (the extinction ratio of light ($I_{max}/I_{min}$) was 50 : 1) because the random lasers emission originated from the multiple scattering of light in the medium.

Except for the polarization behaviour, the optical stability performance of the random lasing action was also tested, which was still an urgent issue for expanding perovskite microlasers to optoelectronic-related applications. Stabilities of the random

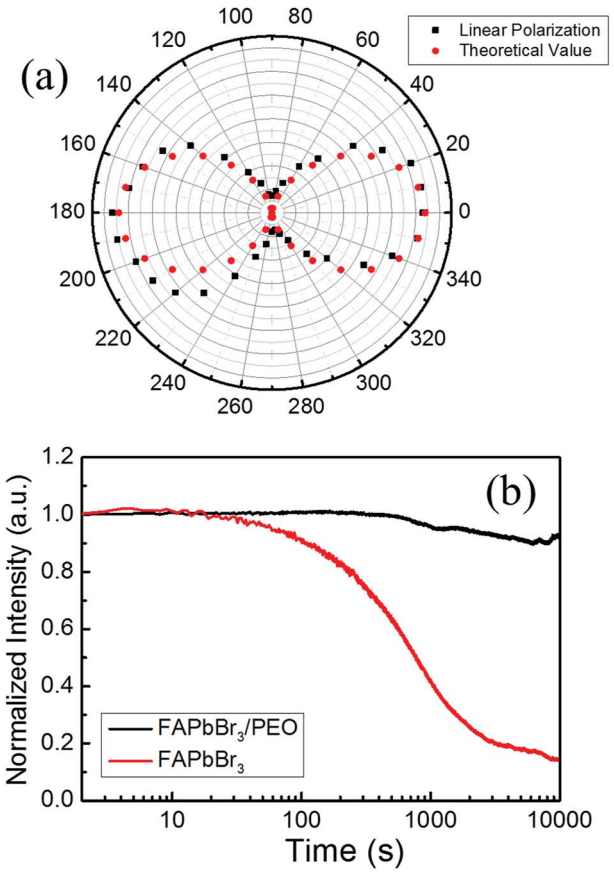


Fig. 4 (a) The polarization property of the lasing emission of $FAPbBr_3$/PEO perovskite thin film; (b) the stability of random lasing emission intensity of $FAPbBr_3$/PEO and the two-photon-pumped photoluminescence of $FAPbBr_3$ perovskite thin films.

lasing emission intensity of $FAPbBr_3$/PEO and two-photon-pumped photoluminescence of $FAPbBr_3$ were tested when exposed to air atmosphere, as seen in Fig. 4(b). The pumping intensity was selected as 1.32 mJ $cm^{-2}$, which was 120% larger than the random lasing emission threshold of $FAPbBr_3$/PEO perovskite nanocrystals. We can see that the two-photon-pumped photoluminescence of $FAPbBr_3$ thin films began damping after 30 seconds (~30 000 shots) under the influence of thermal and moisture effects. Following this, the photoluminescence intensity decreased drastically with time, and reduced to 16% of the original intensity after 10 000 seconds (about $10^7$ shots). While the two-photon-pumped random lasing emission of $FAPbBr_3$/PEO composite thin films showed better stability, the lasing intensity began to fade after 1000 seconds ($10^6$ shots), and 90% of the original intensity was still maintained after 10 000 seconds (about $10^7$ shots), which resulted from the protection of the PEO layer by isolating the $FAPbBr_3$ nanocrystals from moist air. The PEO addictive could separate $FAPbBr_3$ nanocrystals from each other, which increased the thermal dissipation performance effectively. Compared with the large absorption coefficient at the UV and violet regions, the absorption coefficient of $FAPbBr_3$ thin films near the infrared region was almost zero, which may avoid the heat accumulation caused by absorbing the pumping beam.

The enhanced photoluminescence emission intensity in $FAPbBr_3$/PEO composite thin films was promising in developing effective light sources. In addition, the two-photon-pumped photoluminescence of $FAPbBr_3$ thin films pumped at 1064 nm may possess great potential in non-invasive medical treatment because this waveband is not absorbed by the aqueous solution. Moreover, the high stability made the $FAPbBr_3$/PEO composite thin films more valuable in developing continuous-wave pumped lasers and even electrical pumped lasers. These results were also promising in the application of optoelectronic devices.

## Conclusions

Based on all the experimental results mentioned above, we can see that two-photon-pumped random lasing action was achieved in $FAPbBr_3$/PEO composite perovskite thin films based on the multiple scattering of light among the PEO bulks. Although the threshold was much larger than that pumped by UV pulse lasers (several microjoules), it was still comparable to the lasing action in other colloidal quantum dots, inorganic semiconductor nanowires, and other perovskite thin films based on the two-photon-pumped process. More significantly, the enhanced optical stability of lasing action in this study was excited by using a nanosecond pulse laser at room temperature, which laid the foundation for the realization of the microsecond laser for continuous-wave pumping lasers. This study also provided an economical and effective method for enhancing photoluminescence efficiency with higher moisture and thermal stability, which may be desirable for expanding the application of organic perovskite materials in optoelectronic devices.

## Conflicts of interest

The authors declare that they have no conflicts of interest.

## Acknowledgements

This study was financially supported by the National Natural Science Foundation of China (Grant No. 61805206 and 11504300), Fundamental Research Funds for the Central Universities of China (Grant No. XDJK2017C061 and SWU116051), and Chongqing Normal University Funds (Grant No. 18XLB002).

## References

1 J. H. Im, C.-R. Lee, J.-W. Lee, S. W. Park and N.-G. Park, *Nanoscale*, 2011, **3**, 4088–4093.
2 W. S. Yang, J. H. Noh, N. J. Jeon, Y. C. Kim, S. Ryu, J. Seo and S. I. Seok, *Science*, 2015, **348**, 1234–1237.
3 Q. Zhang, M. Kaisti, A. Prabhu, Y. Yu, Y. A. Song, M. H. Rafailovich and K. Levon, *Electrochim. Acta*, 2018, **261**, 256–264.
4 M. Kaisti, Q. Zhang and K. Levon, *Sens. Actuators, B*, 2017, **241**, 321–326.

5 X. Y. Chin, D. Cortecchia, J. Yin, A. Bruno and C. Soci, *Nat. Commun.*, 2015, **6**, 7383.
6 Q. Zhang, H. S. Majumdar, M. Kaisti, A. Prabhu, A. Ivaska, R. Österbacka and K. Levon, *IEEE Int. Electron Devices Meet.*, 2015, **62**(4), 1291–1298.
7 B. R. Sutherland and E. H. Sargent, *Nat. Photonics*, 2016, **10**(5), 295.
8 Z. K. Tan, R. S. Moghaddam, M. L. Lai, P. Docampo, R. Higler, F. Deschler and F. Hanusch, *Nat. Nanotechnol.*, 2014, **9**(9), 687–692.
9 F. Hao, C. C. Stoumpos, D. H. Cao, R. P. Chang and M. G. Kanatzidis, *Nat. Photonics*, 2014, **8**(6), 489.
10 J. M. Frost, K. T. Butler, F. Brivio, C. H. Hendon, M. Van Schilfgaarde and A. Walsh, *Nano Lett.*, 2014, **14**(5), 2584–2590.
11 F. Deschler, M. Price, S. Pathak, L. E. Klintberg, D. D. Jarausch, R. Higler and M. Atatüre, *J. Phys. Chem. Lett.*, 2014, **5**(8), 1421–1426.
12 P. Chen, Z. Xiong, X. Wu, M. Shao, X. Ma, Z. H. Xiong and C. Gao, *J. Phys. Chem. Lett.*, 2017, **8**(8), 1810–1818.
13 L. Protesescu, S. Yakunin, M. I. Bodnarchuk, F. Krieg, R. Caputo, C. H. Hendon and M. V. Kovalenko, *Nano Lett.*, 2015, **15**(6), 3692–3696.
14 C. Wehrenfennig, G. E. Eperon, M. B. Johnston, H. J. Snaith and L. M. Herz, *Adv. Mater.*, 2014, **26**(10), 1584–1589.
15 G. E. Eperon, S. D. Stranks, C. Menelaou, M. B. Johnston, L. M. Herz and H. J. Snaith, *Energy Environ. Sci.*, 2014, **7**(3), 982–988.
16 F. Deschler, M. Price, S. Pathak, L. E. Klintberg, D. D. Jarausch, R. Higler and M. Atatüre, *J. Phys. Chem. Lett.*, 2014, **5**(8), 1421–1426.
17 S. Yakunin, L. Protesescu, F. Krieg, M. I. Bodnarchuk, G. Nedelcu, M. Humer and M. V. Kovalenko, *Nat. Commun.*, 2015, **6**, 8056.
18 L. Dou, Y. M. Yang, J. You, Z. Hong, W. H. Chang, G. Li and Y. Yang, *Nat. Commun.*, 2014, **5**, 5404.
19 G. Y. Kim, A. Senocrate, T. Y. Yang, G. Gregori, M. Grätzel and J. Maier, *Nat. Mater.*, 2018, **17**(5), 445.
20 Z. Yuan, C. Zhou, Y. Tian, Y. Shu, J. Messier, J. C. Wang and K. Schanze, *Nat. Commun.*, 2017, **8**, 14051.
21 N. K. Noel, A. Abate, S. D. Stranks, E. S. Parrott, V. M. Burlakov, A. Goriely and H. J. Snaith, *ACS Nano*, 2014, **8**(10), 9815–9821.
22 U. Mehmood, A. Al-Ahmed, M. Afzaal, F. A. Al-Sulaiman and M. Daud, *Renewable Sustainable Energy Rev.*, 2017, **78**, 1–14.
23 T. Leijtens, K. Bush, R. Cheacharoen, R. Beal, A. Bowring and M. D. McGehee, *J. Mater. Chem. A*, 2017, **5**(23), 11483–11500.
24 Y. Fu, H. Zhu, A. W. Schrader, D. Liang, Q. Ding, P. Joshi and S. Jin, *Nano Lett.*, 2016, **16**(2), 1000–1008.
25 A. Perumal, S. Shendre, M. Li, Y. K. E. Tay, V. K. Sharma, S. Chen and S. T. Tan, *Sci. Rep.*, 2016, **6**, 36733.
26 J. Yan, Y. Chen, J. Wang, A. Zhang and B. Zhang, *Opt. Mater.*, 2017, **73**, 736–741.
27 D. Priante, I. Dursun, M. S. Alias, D. Shi, V. A. Melnikov, T. K. Ng and B. S. Ooi, *Appl. Phys. Lett.*, 2015, **106**(8), 081902.
28 H. Zhu, Y. Fu, F. Meng, X. Wu, Z. Gong, Q. Ding and X. Y. Zhu, *Nat. Mater.*, 2015, **14**(6), 636.
29 S. D. Stranks, S. M. Wood, K. Wojciechowski, F. Deschler, M. Saliba, H. Khandelwal and A. P. Schenning, *Nano Lett.*, 2015, **15**(8), 4935–4941.
30 Q. Liao, K. Hu, H. Zhang, X. Wang, J. Yao and H. Fu, *Adv. Mater.*, 2015, **27**(22), 3405–3410.
31 Q. Zhang, R. Su, X. Liu, J. Xing, T. C. Sum and Q. Xiong, *Adv. Funct. Mater.*, 2016, **26**(34), 6238–6245.
32 R. Dhanker, A. N. Brigeman, A. V. Larsen, R. J. Stewart, J. B. Asbury and N. C. Giebink, *Appl. Phys. Lett.*, 2014, **105**(15), 151112.
33 A. Safdar, Y. Wang and T. F. Krauss, *Opt. Express*, 2018, **26**(2), A75–A84.
34 K. Wang, S. Sun, C. Zhang, W. Sun, Z. Gu, S. Xiao and Q. Song, *Mater. Chem. Front.*, 2017, **1**(3), 477–481.
35 X. Wang, H. Zhou, S. Yuan, W. Zheng, Y. Jiang, X. Zhuang and A. Pan, *Nano Res.*, 2017, **10**(10), 3385–3395.
36 Y. Gao, S. Wang, C. Huang, N. Yi, K. Wang, S. Xiao and Q. Song, *Sci. Rep.*, 2017, **7**, 45391.
37 D. S. Wiersma, *Nat. Phys.*, 2008, **4**(5), 359.
38 X. He, P. Liu, H. Zhang, Q. Liao, J. Yao and H. Fu, *Adv. Mater.*, 2017, **29**(12), 1604510.
39 P. Liu, X. He, J. Ren, Q. Liao, J. Yao and H. Fu, *ACS Nano*, 2017, **11**(6), 5766–5773.